A-803467, a potent and selective $Na_v1.8$ sodium channel blocker, attenuates neuropathic and inflammatory pain in the rat

Michael F. Jarvis*†, Prisca Honore*, Char-Chang Shieh*, Mark Chapman‡, Shailen Joshi*, Xu-Feng Zhang*, Michael Kort*, William Carroll*, Brian Marron‡, Robert Atkinson‡, James Thomas‡, Dong Liu‡, Michael Krambis‡, Yi Liu‡, Steve McGaraughty*, Katharine Chu*, Rosemarie Roeloffs‡, Chengmin Zhong*, Joseph P. Mikusa*, Gricelda Hernandez*, Donna Gauvin*, Carrie Wade*, Chang Zhu*, Madhavi Pai*, Marc Scanio*, Lei Shi*, Irene Drizin*, Robert Gregg*, Mark Matulenko*, Ahmed Hakeem*, Michael Gross‡, Matthew Johnson‡, Kennan Marsh*, P. Kay Wagoner‡, James P. Sullivan*, Connie R. Faltynek*, and Douglas S. Krafte‡§

*Neuroscience Research, Abbott Laboratories, Abbott Park, IL 60064; and ‡Icagen, Inc., Durham, NC 27703

Edited by William A. Catterall, University of Washington School of Medicine, Seattle, WA, and approved March 25, 2007 (received for review December 20, 2006)

Activation of tetrodotoxin-resistant sodium channels contributes to action potential electrogenesis in neurons. Antisense oligonucleotide studies directed against $Na_v1.8$ have shown that this channel contributes to experimental inflammatory and neuropathic pain. We report here the discovery of A-803467, a sodium channel blocker that potently blocks tetrodotoxin-resistant currents (IC_{50} = 140 nM) and the generation of spontaneous and electrically evoked action potentials *in vitro* in rat dorsal root ganglion neurons. In recombinant cell lines, A-803467 potently blocked human $Na_v1.8$ (IC_{50} = 8 nM) and was >100-fold selective vs. human $Na_v1.2$, $Na_v1.3$, $Na_v1.5$, and $Na_v1.7$ (IC_{50} values ≥1 μM). A-803467 (20 mg/kg, i.v.) blocked mechanically evoked firing of wide dynamic range neurons in the rat spinal dorsal horn. A-803467 also dose-dependently reduced mechanical allodynia in a variety of rat pain models including: spinal nerve ligation (ED_{50} = 47 mg/kg, i.p.), sciatic nerve injury (ED_{50} = 85 mg/kg, i.p.), capsaicin-induced secondary mechanical allodynia (ED_{50} ≈ 100 mg/kg, i.p.), and thermal hyperalgesia after intraplantar complete Freund's adjuvant injection (ED_{50} = 41 mg/kg, i.p.). A-803467 was inactive against formalin-induced nociception and acute thermal and postoperative pain. These data demonstrate that acute and selective pharmacological blockade of $Na_v1.8$ sodium channels *in vivo* produces significant antinociception in animal models of neuropathic and inflammatory pain.

allodynia | electrophysiology | hyperalgesia | sensory neurons

The excitability of peripheral nerves is governed by the expression of voltage-gated sodium channels (1). Certain tetrodotoxin-resistant (TTX-R) sodium channels have high activation thresholds, slow inactivation kinetics, and channel opening leads directly to the generation of action potentials (2, 3). $Na_v1.8$ is a TTX-R sodium channel with these properties and is highly expressed in small-diameter sensory neurons (4, 5). The expression and biophysical properties of $Na_v1.8$ channels can be modulated by ongoing nociceptive input. For example, there is increased $Na_v1.8$ channel expression in the rat digital nerve and dorsal root ganglion (DRG) after intraplantar administration of complete Freund's adjuvant (CFA) or carrageenan (CARR), respectively (6, 7). Similarly, local administration of prostaglandin-E2, adenosine, or serotonin produces an increase in TTX-R sodium current magnitude in peripheral nerves through modulation of the voltage-dependent properties of $Na_v1.8$ and other sodium channels (8–10). Direct nerve injury (e.g., L5/L6 spinal nerve ligation) also leads to immunocytochemical and electrophysiological changes in $Na_v1.8$ channels suggesting a potential role for this channel in the sensation of neuropathic pain (11). Human patients with chronic neurogenic pain or chronic local hyperalgesia also show increased $Na_v1.8$ channel expression proximal to a peripheral injury site (12–14).

In the absence of subtype selective sodium channel blockers, $Na_v1.8$ knockout mice have provided insights for the specific role of $Na_v1.8$ channels in pain states (15–18). These mice do not express $Na_v1.8$-mediated TTX-R currents in DRG neurons and show a decreased sensitivity to mechanical stimuli and delayed development of thermal hyperalgesia. However, interpretation of the $Na_v1.8$ knockout phenotype has been complicated by a compensatory increased expression of other sodium channel subtypes (19). In addition, nociceptor-specific knockout of $Na_v1.8$ and another sodium channel did not prevent the development of neuropathic pain in the mouse (20).

Additional evidence for $Na_v1.8$ involvement in transduction of nociceptive information was derived from studies using antisense (AS) oligodeoxynucleotides (ODNs) (11, 21–23). Selective knockdown of $Na_v1.8$ protein after $Na_v1.8$ AS ODN treatment reversed mechanical allodynia and thermal hyperalgesia after peripheral inflammation and nerve injury (22, 24). This $Na_v1.8$ knockdown strategy has also demonstrated $Na_v1.8$ involvement in afferent nerve sensitization after chemical irritation of the bladder and visceral pain (23). Collectively, these findings strongly support a key role for $Na_v1.8$ in regulating the properties of nociceptive neurons and, consequently, nociceptive behaviors.

Although it is widely appreciated that blockade of sodium channels contributes to the analgesic activity of a large number of nonopioid analgesics like lamotrigine and amitriptyline (19, 25, 26), the identification of specific blockers of individual sodium channels

Author contributions: M.F.J., P.H., C.-C.S., M. Kort, W.C., B.M., R.K.W., J.P.S., C.R.F., and D.S.K. designed research; P.H., C.-C.S., M.C., S.J., X.-F.Z., R.A., J.T., D.L., M. Krambis, Y.L., S.M., K.C., R.R., C. Zhong, J.P.M., G.H., D.G., C.W., C. Zhu, M.P., M.S., L.S., I.D., R.G., M.M., A.H., M.G., M.J., and K.M. performed research; M. Kort, W.C., B.M., R.A., J.T., M.S., I.D., R.G., L.S., M.M., A.H., M.G., and M.J. contributed new reagents/analytic tools; M.F.J., P.H., C.-C.S., M.C., S.J., S.M., K.M., P.K.W., J.P.S., C.R.F., and D.S.K. analyzed data; and M.F.J., P.H., and D.S.K. wrote the paper.

Conflict of interest statement: All authors are employees of either Abbott Laboratories or Icagen, Inc.

This article is a PNAS Direct Submission.

Abbreviations: CARR, carrageenan; CFA, complete Freund's adjuvant; DRG, dorsal root ganglion; TTX, tetrodotoxin; TTX-R, TTX-resistant; WDR, wide dynamic range.

See Commentary on page 8205.

†To whom correspondence may be addressed at: Abbott Laboratories, R-4PM, AP9A/3,100 Abbott Park Road, Abbott Park, IL 60064. E-mail: michael.jarvis@abbott.com.

§To whom correspondence may be addressed at: Icagen, Inc., P.O. Box 14487, Research Triangle Park, NC 27709. E-mail: dkrafte@icagen.com.

This article contains supporting information online at www.pnas.org/cgi/content/full/0611364104/DC1.

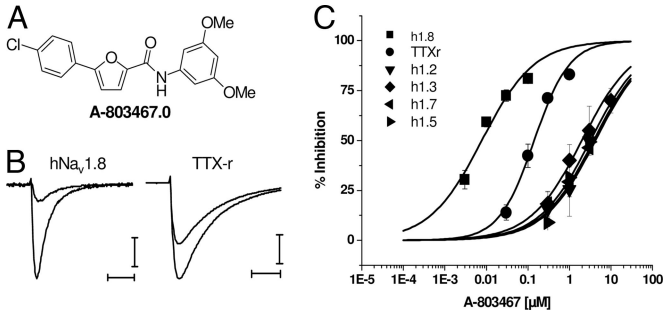

Fig. 1. A-803467 is a selective blocker of $Na_V1.8$ channels. (*A*) Chemical structure of A-803467. (*B*) Block of recombinant and native $Na_V1.8$ currents by 100 nM A-803467. Current records were generated during voltage steps to 0 mV in control and after application of A-803467 (100 nM) for human $Na_V1.8$ or native DRG TTX-R currents. Holding potentials were set at −100 mV, and each test pulse was preceded by an 8-s prepulse to −40 mV, followed by 20 ms at −100 mV before a 20-ms depolarization to 0 mV. [Scale bars, 0.3 nA and 5 ms ($Na_V1.8$) and 1.5 nA and 5 ms (TTX-R).] (*C*) Representative concentration–response curves were generated after application of different concentrations of A-803467 and assessment of current block for human $Na_V1.8$ (IC_{50} = 8 ± 1 nM), and TTX-R currents (IC_{50} = 140 ± 14 nM) in rat DRG cells and $hNa_V1.2$, $hNa_V1.3$, $hNa_V1.5$, and $hNa_V1.7$. Data represent means ± SEM from at least three separate experiments. Percent inhibition was calculated as 1 − (test current/(control current + wash current/2)) and plotted vs. test concentration. Concentration-effect curves were fit by using the Hill equation to estimate IC_{50} values and Hill coefficients. For $hNa_V1.2$, 1.3, 1.5, and 1.7, Hill coefficients were set to 0.7 as was found for $Na_V1.8$. Holding potentials for selectivity targets were −60 mV for $hNa_V1.2$, 1.3, and 1.7 and −90 mV for $hNa_V1.5$.

has remained challenging (19). The present studies were undertaken to characterize the antinociceptive effects of A-803467 (Fig. 1*A*), a sodium channel blocker that has high affinity and selectivity for blocking human $Na_V1.8$ channels. A-803467 effectively inhibited spontaneous and evoked neuron firing in both *in vitro* and *in vivo* electrophysiological preparations and dose-dependently reduced nociception in neuropathic and inflammatory pain models.

Results and Discussion

The discovery of A-803467 resulted from an extensive structure-activity relationship study of chemically novel blockers of TTX-R currents in rat DRG neurons. The furan–amide series was identified from an iterative screening strategy that focused on both affinity and selectivity for block of $Na_V1.8$. Like other sodium channel blockers such as local anesthetics (19, 26), many of these compounds showed preferential affinity for inactivated states of the channel (2, 3). Active analogs were tested in electrophysiological assays to assess interactions with human $Na_V1.8$ and then further profiled for selectivity against other sodium channels and various receptors.

A-803467 Blocks Recombinant Human and Native Rat $Na_V1.8$ Currents. The application of 100 nM A-803467 to either TTX-R currents from rat dorsal root ganglion neurons or HEK-293 cells expressing human $Na_V1.8$ sodium channels produced significant current block (Fig. 1*B*). Because the biophysical properties vary among sodium channel subunits (2, 3), electrophysiological protocols were designed to set the membrane potential to the midpoint of voltage-dependent steady-state inactivation (i.e., the voltage at which 50% of channels are inactivated) or to a voltage that sets all channels in a resting state to allow a direct comparison of compound effects across channel subtypes (Table 1). A-803467 produced a concentration-dependent (IC_{50} = 140 nM) block of TTX-R currents in small diameter (18–25 μm) rat dorsal root ganglion neurons at a holding potential of −40 mV (Fig. 1*C*). Data are also shown for other recombinant sodium channels to illustrate selectivity. Under these conditions, both mexiletine and lamotrigine also blocked

Table 1. A-803467 selectively blocks human $Na_V1.8$ sodium channels

	IC_{50}, μM	
	V_0*	$V_{1/2}$†
$hNa_V1.8$	0.079 ± 0.01	0.008 ± 0.002
$hNa_V1.2$	9.49 ± 0.23	7.38 ± 0.17
$hNa_V1.3$	11.76 ± 0.91	2.45 ± 0.05
$hNa_V1.5$	32.82 ± 4.89	7.34 ± 0.21
$hNa_V1.7$	35.34 ± 0.30	6.74 ± 0.03

*Resting state protocol: the prepulse voltage at which 100% of channels are available to be activated. (V_0 = −100 mV for $hNa_V1.8$; V_0 = −120 mV for $hNa_V1.2$, $hNa_V1.3$, $hNa_V1.7$; V_0 = −150 mV for $hNa_V1.5$.)

†Inactivated state protocol: the prepulse voltage at which 50% of channels are inactivated. ($V_{1/2}$ = −40 mV for $hNa_V1.8$; $V_{1/2}$ = −60 mV for $hNa_V1.2$, $hNa_V1.3$, $hNa_V1.7$; $V_{1/2}$ = −90 mV for $hNa_V1.5$.)

TTX-R currents with IC_{50} values of >30 μM (data not shown). Small-diameter DRG neurons express at least two subtypes of TTX-R currents, $Na_V1.8$ and $Na_V1.9$ (27, 28). Under the present experimental conditions, the contribution of $Na_V1.9$ to the peak current evoked at 0 mV was minimal (27) (M.C., unpublished observations). At a resting state, A-803467 also potently blocked human $Na_V1.8$ channels (IC_{50} = 79 nM, Table 1). The IC_{50} value for A-803467 to block human $Na_V1.8$ channels was 8 nM at a holding potential (−40 mV) that gives half-maximal inactivation (Fig. 1*C*). A-803467 also potently blocked recombinant rat $Na_V1.8$ channels (IC_{50} = 45 ± 5 nM) at a holding potential of −40 mV. The apparent difference in the potency of A-803467 to block recombinant rat compared with human $Na_V1.8$ channels likely reflects direct interactions with the α-subunit. Smaller shifts from recombinant rat channels to TTX-R in DRG neurons may reflect modulation by accessory subunits in native versus recombinant cell systems.

Further characterization of the ability of A-803467 to block $Na_V1.8$ channels showed that this compound effectively reduced recombinant human $Na_V1.8$-mediated currents at all holding potentials. The relationship between channel block and membrane potential is illustrated in Fig. 2*A*, where the degree of block is shown after prepulses to various voltages. Even at negative potentials (e.g., −100 mV), >50% of the maximal current was blocked by 0.3 μM A-803467, indicating block of the resting channel. IC_{50} values generated for $Na_V1.8$ channel block after negative prepulse potentials were typically greater than those from −40 mV, possibly reflecting lower-affinity interactions with the channels at resting states. Similar to its activity at human $Na_V1.8$ channels, A-803467 was less potent at more negative membrane potentials against native TTX-R currents (IC_{50} = 1 μM, −100 mV prepulse). There were, however, also qualitative differences, in that little to no block was observed after more negative prepulses. This may reflect a 10-fold shift in potency as observed in the recombinant system due to less interaction with the resting states of the channel in native cells.

To assess possible interactions with additional states or conformations of the channel, normalized steady-state inactivation curves are shown in Fig. 2*B*. The $V_{1/2}$ value for steady-state inactivation shifted from −50 ± 5 mV in control to −63 ± 2 mV with 0.3 μM and −60 ± 6 mV with 1 μM A-803467. Although additional concentration-dependent channel block was observed at negative membrane potentials, the shift in $V_{1/2}$ values appeared to saturate within the resolution of our analysis at concentrations ≤0.3 μM, consistent with an effect on the resting state of the channel (i.e., K_r). The effects of A-803467 were reversible (Fig. 2 *A* and *B*), indicating run down or time-dependent shifts in voltage-dependent properties did not affect the results. These data demonstrate that A-803467 preferentially inhibits inactivated channels, although there is significant block from the resting state in recombinant systems. Shifts

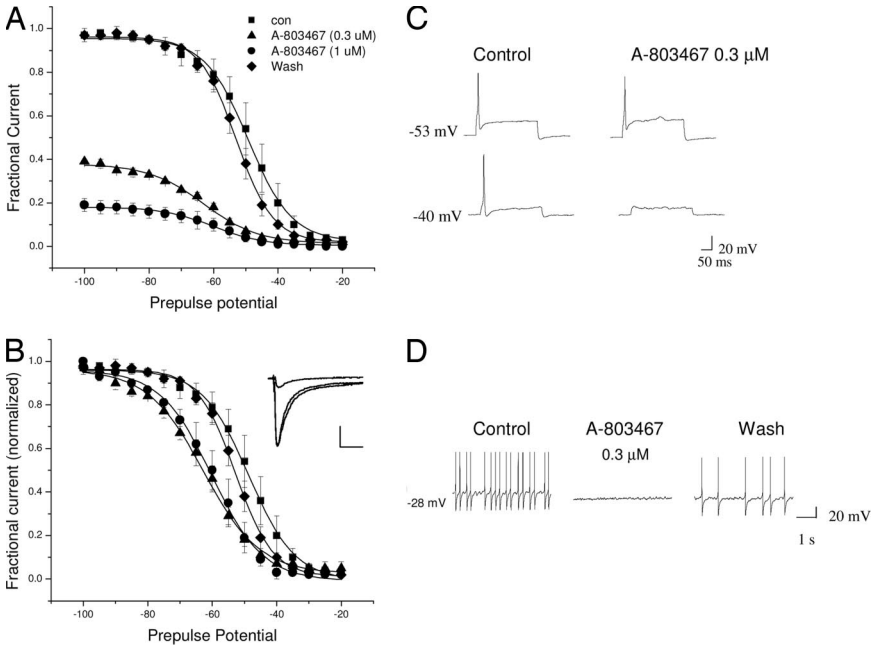

Fig. 2. Voltage-dependent block and shifts in steady-state inactivation of $Na_v1.8$ currents by A-803467. Block of recombinant $hNa_v1.8$ currents by A-803467 was assessed after voltage protocols designed to vary the level of steady-state inactivation. Holding potential was −100 mV, and 500-ms prepulses were given to various potentials, followed by a 20-ms step to 0 mV. A 20-ms gap at −100 mV separated prepulse from test pulse. (*A*) Fractional current plotted against prepulse potential. Current values were normalized to the maximal current observed in control after prepulses to −100 mV. (*B*) Normalized fractional current vs. prepulse potential to illustrate shifts in $V_{1/2}$ values observed in the presence of drug. The current inset illustrates control, 1 μM A-803467, and recovery (e.g., wash) values. The smaller current record is in the presence of test compound. Symbols are the same as for *A*. Curve fits in both panels were derived by fitting Boltzmann equations to the data to obtain $V_{1/2}$ and slope factors (normalized current = $[1 + \exp[(V - V_{1/2})/k]^{-1}$ where V is the prepulse potential, $V_{1/2}$ is the holding potential that gave half-maximal inactivation, and *k* is the slope factor). [Scale bars, 0.5 nA and 5 msec ($Na_v1.8$).] Data represent means ± SEM from at least three separate experiments. (*C* and *D*) Effects of A-803467 on action potential firing in DRG neurons. Action potentials were recorded from small-diameter (18–25 μm) DRG neurons obtained from vehicle- or CFA-treated animals. (*C*) Action potentials were evoked in DRG neurons by injecting threshold current ranging from 100 to 300 pA from a resting state (resting membrane potential of ≈−53 mV, no current injection) or a depolarized state (−40 mV, by injecting 20- to 30-pA current). Evoked action potentials from resting state are not sensitive to 300 nM A-803467, which completely blocks evoked action potential from a depolarized state (representative of $n = 4$). A-803467 at 100 nM was ineffective in blocking evoked action potentials from both resting and depolarized states (data not shown). (*D*) Spontaneously firing neurons were obtained from small-diameter DRG neurons isolated 48 h after intraplantar CFA injection into the rat hindpaw. Approximately 10–12% of the neurons from CFA-treated animals fire spontaneously in our experiments. Representative responses ($n = 4$) are shown for control after application of 300 nM A-803467 and after wash out.

of comparable magnitude in $V_{1/2}$ values were also observed in the DRG neurons, consistent with interaction with inactivated states of the channel in a native system. No effects were seen on the voltage-dependence of activation (data not shown). Additionally, A-803467 did not show significant frequency-dependent block in either native neurons or recombinant cells [see supporting information (SI)]. The lack of frequency-dependent block is atypical for small-molecule sodium channel blockers, but a consistent property of this chemotype.

A-803467 Selectively Blocks $Na_v1.8$. The activity of A-803467 to block other sodium channels was evaluated at approximate half-maximal inactivation holding potentials and at voltages where all channels should be in the resting state before the voltage step (Table 1). A-803467 was 300- to 1,000-fold more potent at blocking $Na_v1.8$ as compared with its ability to block $Na_V1.2$, $Na_V1.3$, $Na_V1.5$, and $Na_V1.7$ under these conditions (Table 1). A-803467 was also tested against other channels and receptors expressed in peripheral sensory neurons including TRPV1, $P2X_{2/3}$, $Ca_v2.2$ calcium channels, and KCNQ2/3 potassium channels. A-803467 did not show significant activity at these channels ($IC_{50} > 10$ μM). In addition, A-803467 was evaluated in a broad screening panel ($n = 81$) of cell-surface receptors, ion channels, and enzymes (CEREP, Poitiers, France) and showed no or weak activity ($IC_{50} > 2$ μM) at these targets (see SI).

A-803467 Suppresses Evoked and Spontaneous DRG Neuronal Action Potentials. The biophysical properties of A-803467 to block $Na_v1.8$ channels indicate that this selective $Na_v1.8$ blocker should inhibit action potential firing, in a voltage-dependent fashion, in those DRG neurons where TTX-R currents play a prominent role. At 0.3 μM, A-803467 produced little effect on evoked action potential firing (single spikes) when small diameter DRG neurons had a resting potential at −55 mV or below (Fig. 2*C*). However, when the same neuron resting potential was more depolarized (≈−40 mV), A-803467 (0.3 μM) effectively suppressed evoked action potential firing. A-803467 did not block action potential firing at a concentration of 0.1 μM. To determine whether A-803467 can also suppress ectopic neuronal firing, which contributes to the pain signaling transduction in neuropathic or inflammatory pain (19, 28), the effect of A-803467 on the spontaneous firing of isolated DRG neurons was examined 2 days after CFA-induced inflammation (29). As shown in Fig. 2*D*, application of A-803467 (0.3 μM) reversibly suppressed the spontaneous firing of small diameter DRG neurons.

Pharmacokinetic Profile of A-803467. A-803467 had moderate bioavailability ($F = 26\%$) after i.p. administration of 10 mg/kg with a C_{max} of 0.35 μg/ml and a T_{max} of 1.6 h (see SI). Plasma samples harvested 45 min after administration of A-803467 in the dose range of 10 to 100 mg/kg, i.p. generated total plasma concentrations in the range of 0.4 to 7.0 μg/ml. A-803467 was very highly bound (98.7%) to plasma proteins in the rat. Free plasma concentrations of A-803467 that provided robust (≥70%) analgesic efficacy in a spinal nerve ligation model were in the range of 200–300 nM that were ≈1.5- to 3-fold greater than the rat DRG TTX-R IC_{50} value.

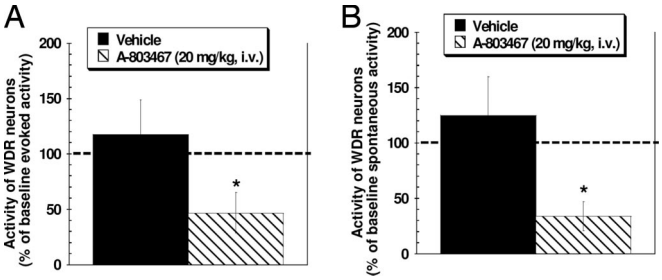

Fig. 3. Administration of A-803467 (20 mg/kg, i.v.) significantly reduced von Frey hair-evoked (10 g) (*A*) and spontaneous spinal dorsal horn WDR neuronal (*B*) activity. Discharge activity was recorded from 13 WDR neurons located 756.3 ± 71.7 μm from the surface of the spinal cord in L5/L6 spinal nerve-injured rats. Before A-803467 injection, spontaneous WDR firing (first 5 min) was 2.8 ± 0.8 spikes per second, and the baseline evoked response (von Frey hair, 10 g) was 198 ± 32.9 spikes in 15 s. Administration of A-803467 (20 mg/kg, i.v.) reduced both evoked and spontaneous WDR neuron firing by 66.2% and 53.3%, respectively, from baseline levels. The effects of A-803467 were dose-dependent (data not shown). Data shown were collected 35 min after injection. n = 6–7 per group, *, $P < 0.05$ vs. baseline activity.

Antinociceptive Activity of A-803467. Consistent with its effects on neuronal action potential electrogenesis *in vitro*, systemic administration of A-803467 (20 mg/kg, i.v.) to spinal nerve ligated rats, significantly reduced both spontaneous and von Frey hair-evoked firing of spinal dorsal horn wide dynamic range neurons by 66% and 53%, respectively compared with baseline levels (Fig. 3). These effects were dose-dependent (data not shown). These *in vivo* electrophysiology data demonstrate that systemic delivery of A-803467 alters the activity of spinal sensory neurons after nerve injury.

A-803467 was evaluated in a variety of animal pain models after i.p. administration (Table 2). A-803467 potently attenuated mechanical allodynia in two models of neuropathic pain, the L5/L6 spinal nerve injury model and the chronic constriction injury (CCI) of the sciatic nerve model (Fig. 4, Table 2, and SI). For comparison, gabapentin (ED_{50} = 40 mg/kg) and lamotrigine (ED_{50} = 20 mg/kg) also reduced mechanical allodynia in these models (24). Interestingly, A-803467 also attenuated cold allodynia in the CCI model, but did not significantly reduce mechanical allodynia in the vincristine model of chemotherapy-induced neuropathic pain (Table 2). Capsaicin-induced secondary mechanical allodynia is a potential surrogate assay for clinical and experimental neuropathic pain (30). Similar to its activity in the mechanical nerve injury models, A-803467 significantly decreased allodynia in this assay in a dose-related manner (Fig. 5*A* and Table 2). However, it was inactive at reducing mechanical allodynia observed 2 h after surgery in the skin-incision model of postoperative pain and showed a small, but significant, analgesic effect 24 h after surgery (Table 2).

A-803467 potently reduced thermal hyperalgesia in the CFA model of inflammatory pain (Fig. 5*B* and Table 2). A-803467 was equally effective when given either 2 or 4 days after CFA administration. Under the same conditions, A-803467 had no effect on paw withdrawal latency of the contralateral noninflamed paw, indicative of a specific antihyperalgesic effect in this model (Fig. 5*B*). The antinociceptive effects of A-803467 at Day 4 after CFA are in close agreement with the reported effects of $Na_v1.8$ antisense oligonucleotide treatment (11, 24). A-803467 also significantly reduced CFA-induced mechanical allodynia. A-803467 reduced thermal hyperalgesia in the CARR model of acute inflammatory pain but was not effective in reducing nociception in the persistent phase for the formalin test. (Table 2). Gabapentin and lamotrigine also effectively reduced hyperalgesia in the CFA model (see SI).

Balloon distension of the distal colon/rectum is a model of acute visceral pain (31). A-803467 produced a dose-related analgesic effect in this model. A-803467 also effectively attenuated acetic acid-induced abdominal constrictions in mice (Table 2). These data indicate that A-803467 effectively reduces acute visceral nociceptive responses, however, a similar antinociceptive effect was not observed in the cyclophosphamide model of cystitis-induced inflammatory visceral pain (Table 2). A-803467 significantly decreased acute mechanical but not thermal somatic nociception (Table 2).

A-803467 did not significantly ($P > 0.05$) alter either motor function assessed by spontaneous exploratory behavior or motor

Table 2. Analgesic activity of A-803467

Pain model	ED_{50}	Effect, %
Acute nociception		
Rat acute therm.	>100	0 ± 0
Rat acute mech.	65	70 ± 4*
Inflammatory pain		
Formalin-flinching	>100	9 ± 11
Capsaicin, mech. allodynia	100	46 ± 4*
CARR, therm. hyperalgesia	100	54 ± 10*
CFA, therm. hyperalgesia Day 2	41	64 ± 6*
CFA, therm. hyperalgesia Day 4	38	71 ± 10*
CFA, mech. allodynia Day 2	>100	34 ± 15*
CFA, mech. allodynia Day 4	>100	42 ± 15*
Neuropathic pain		
SNL, mech. allodynia	47	70 ± 12*
CCI, mech. allodynia	85	56 ± 10*
CCI, cold allodynia	70	61 ± 11*
Vincristine, mech. allodynia	>100	9 ± 9
Postoperative pain		
Skin incision at 2 h	>100	14 ± 2
Skin incision at 24 h	>100	32 ± 18*
Visceral pain		
Mouse writhing assay (s.c.)	>100	34 ± 6*
Cyclophosphamide, cystitis	>100	0 ± 10
Colonic distension (MED)	100	25 ± 5*
Motor effects†		
Locomotor activity	>300	12 ± 12
Rotorod performance	>300	0 ± 0
Edge balance	>300	0 ± 0

Percent analgesic effect assessed at 100 mg/kg, i.p. *, significantly different ($P < 0.05$) from vehicle-treated animals (n = 6–12 per experimental group). †, percent effect tested at 300 mg/kg, i.p. therm., thermal; mech., mechanical; MED, minimum effective dose; CCI, chronic constriction injury, SNL, spinal nerve ligation.

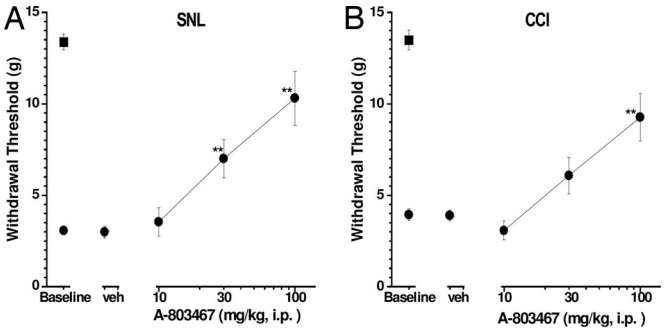

Fig. 4. Antiallodynic effects of A-803467 in neuropathic pain. Two weeks after L5-L6 spinal nerve injury (SNL; *A*) or chronic constriction injury (CCI; *B*) A-803467 was injected 30 min (i.p.) before testing. A-803467 demonstrated significant antiallodynic effects in both neuropathic pain models [*A*: $F(4, 65)$ = 21.94, $P < 0.0001$; *B*: F (4, 42) = 11.75, $P < 0.0001$). Circles represent paw withdrawal threshold ipsilateral to the injury; squares represent paw withdrawal threshold contralateral to the injury. Data represent mean ± SEM. **, $P < 0.01$ as compared with vehicle-treated animals. (n = 6–12 per group).

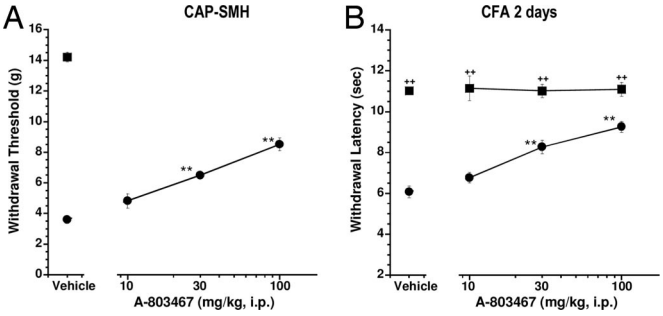

Fig. 5. Antinociceptive effects of A-803467 in the capsaicin-induced secondary mechanical hypersensitivity and CFA-induced thermal hyperalgesia models. A-803467 was injected 30 min (i.p.) before testing in both assays. (*A*) A-803467 reversed the secondary mechanical hypersensitivity tested 3 h after intraplantar capsaicin injection [F (4, 43) = 133.9, $P < 0.001$)]. (*B*) A-803467 demonstrated significant antihyperalgesic effects when tested 2 days after CFA injection [F (7, 40) = 43.74, $P < 0.0001$]. Circles represent values ipsilateral to the injury; squares represent values contralateral to the injury. Data represent mean ± SEM. (n = 6–12 per group). *, $P < 0.05$, **, $P < 0.01$ as compared with vehicle-treated animals. ++, $P < 0.01$ as compared with ipsilateral paw.

coordination and balance as assessed by the rotarod and edge test assays at doses up to 300 mg/kg, i.p. (Table 2).

The present data show that A-803467 is both a potent and highly selective blocker of $Na_v1.8$ sodium channels. To our knowledge, this is the first demonstration of a small-molecule blocker of sodium channels showing both high potency and significant subtype-selectivity among the sodium channel family. Consistent with its activity at recombinant human $Na_v1.8$ channels and at isolated rat DRG neurons, A-803467 effectively blocked both evoked and spontaneous neuronal action potentials *in vitro*. A-803467 also significantly attenuated the firing of spinal dorsal horn neurons *in vivo*. After systemic administration, A-803467 demonstrated dose-dependent antinociceptive effects in experimental pain models. Collectively, these data provide direct evidence that activation of $Na_v1.8$ channels is a major contributor to neuronal action potential generation and to ongoing nociception after peripheral inflammation and nerve injury.

A-803467 potently blocked human $Na_v1.8$ channels in both the resting and inactivated states. Whereas A-803467 showed preferential affinity for inactivated channels, A-803467 did not show significant frequency-dependence in its ability to block $Na_v1.8$ as has been shown for nonselective sodium channel blockers (19). A-803467 also potently blocked native rat TTX-R currents as well as spontaneous and electrically evoked action potentials in rat DRG neurons in a similar fashion. Although the exact mechanism by which A-803467 selectively blocks $Na_v1.8$ channels remains to be investigated, the present data indicate that A-803467 may bind to $Na_v1.8$ at a different site as compared with previously described nonselective sodium channel blockers (19, 26) or at least interacts with the local anesthetic-binding site in a unique manner.

$Na_v1.8$ sodium channels contribute substantially to the inward current during action potential generation in small-diameter sensory neurons (5). Both genetic knockout and antisense knockdown studies have implicated a role for $Na_v1.8$ in different pain states. $Na_v1.8$ gene-disrupted mice show reduced inflammatory hyperalgesia relative to wild-type controls; however, this interpretation is complicated by an up-regulation of TTX-sensitive channels in the knockout mice (15). $Na_v1.8$ antisense studies have provided further evidence that this channel contributes to neuropathic (22, 24), inflammatory (11, 22, 24), and visceral (23) pain. Because a number of different peripheral nerve sodium channel subtypes including $Na_v1.3$, $Na_v1.7$, $Na_v1.8$, and $Na_v1.9$ have been implicated in the processing of nociceptive information (19), it is interesting that the analgesic profile of A-803467 in experimental pain models is highly consistent with the $Na_v1.8$ antisense data. After systemic administration, A-803467 was most effective in reducing pain in models of nerve injury and inflammation-induced pain. Interestingly, neither A-803467, nor specific $Na_v1.8$ antisense treatment (24) produced antinociceptive effects in a chemotherapy-induced pain model (vincristine), suggesting that the role of $Na_v1.8$ channels in this neuropathic pain model may be less than that after mechanical nerve injury. A-803467 also effectively reduced capsaicin-induced mechanical allodynia, a model that may be predictive of analgesic activity in neuropathic pain states (30).

A-803467 attenuated pain sensitivity associated with acute and subchronic inflammatory pain as well as acute visceral pain. However, the analgesic effects of A-803467 were not equivalent across all pain models indicating that activation of $Na_v1.8$ channels may differentially mediate some forms of nociceptive sensory processing or that other sodium channels contribute to nociceptive input only in specific pain states. The ability of A-803467 to reduce neuropathic pain also agrees with previous reports that nonselective sodium channel blockers are active in these models (32, 33). Interestingly, A-803467, which shows good penetration into the central nervous system, produced more robust antinociception in neuropathic pain models than a peripherally acting nonselective sodium channel blocker (32). The ability of A-803467 to suppress spinal dorsal horn neuronal excitability and to effectively reduce allodynia after nerve injury provide further evidence that activation of $Na_v1.8$ channels in peripheral nerves, with synaptic connections in the spinal cord, represents an important site of nociceptive sensory processing (34).

Although lacking analgesic effects on acute thermal pain in normal rats, A-803467 significantly decreased acute mechanical nociception. This effect is in agreement with previous knockout and antisense data demonstrating that knockdown of $Na_v1.8$ was associated with decreased acute mechanical nociception. More than 50% of C fibers and 10% of A fibers express $Na_v1.8$ channels (35). The $Na_v1.8$-positive C fibers are NGF- or GDNF-responsive, and many of these fibers also express TRPV1, supporting a role in acute thermal nociception (35). However, the expression of $Na_v1.8$ channels on A-fibers and the data showing that disruption of $Na_v1.8$ function reduces acute mechanical nociception provide evidence that activation of $Na_v1.8$ channels contributes to normal sensitivity to noxious mechanical stimulation.

In summary, the present data demonstrate that A-803467 is a potent and highly selective blocker of $Na_v1.8$ channels and that this compound effectively blocks sensory neuron excitability *in vitro* and *in vivo*. Evaluation of A-803467 in a wide range of animal pain models demonstrates that selective blockade of $Na_v1.8$ channels *in vivo* results in a significant reduction in nociceptive sensitivity after nerve injury and inflammation.

Materials and Methods

Subjects. In most experiments, male Sprague–Dawley rats (Charles River, Wilmington, MA) weighing 200–300 g were used. The abdominal constriction assay was conducted by using male CD1 mice weighing 20–25 g (Charles River). All animals were group-housed in Association for Assessment and Accreditation of Laboratory Animal Care-approved facilities at Abbott Laboratories in a temperature-regulated environment with lights on between 0700 and 2000 h. Food and water was available ad libitum except during testing. All animal handling and experimental protocols were approved by an institutional animal care and use committee. All experiments were performed during the light cycle.

Electrophysiology. ***Rat DRG neurons.*** Whole-cell patch clamp recordings were performed on rat small diameter DRG neurons (18–25 μm) from the L4 and L5 lumbar region at room temperature as previously described (29). For current clamp recordings, the pipette solution contained 140 mM KCl, 2 mM $MgCl_2$, 5 mM EGTA, and 10 mM Hepes, pH 7.2 (osmolarity, 285). The external solution

contained 140 mM NaCl, 5 mM KCl, 2 mM $CaCl_2$, 2 mM $MgCl_2$, and 10 mM Hepes, pH 7.4 (osmolarity, 310). For voltage-clamp recordings, pipette solution contained 135 mM CsF, 5 mM NaCl, 10 mM CsCl, 5 m MEGTA, and 10 mM Hepes, pH 7.2 (osmolarity, 285). The external solution contained 0.0005 mM TTX, 22 mM NaCl, 110 mM CholineCl, 1.8 mM $CaCl_2$, 0.8 mM $MgCl_2$, 0.05 mM $CdCl_2$, 10 mM Hepes, and 5 mM Glucose, pH 7.4 (osmolarity, 310).

Recombinant human sodium channels. HEK-293 cells expressing recombinant sodium channels were grown in DMEM/high-glucose Dulbecco's modified, 10% FBS, 2 mM sodium pyruvate, and G418. For whole-cell voltage-clamp recordings, patch pipettes were pulled from borosilicate glass on a Flaming-Brown micropipette puller (Sutter Instruments, Novato, CA). Pipettes had a tip resistance of 0.8–2.5 MΩ with the internal solutions 135 mM CsF, 10 mM CsCl, 5 mM EGTA, 5 mM NaCl, 10 mM Hepes, pH to 7.3, with 5 M CsOH, and voltage offset was zeroed before seal formation. The external buffer consisted of 132 mM NaCl, 5.4 mM KCl, 0.8 mM $MgCl_2$, 1.8 mM $CaCl_2$, 5 mM Glucose, and 10 mM Hepes-free acid, pH to 7.3, with 6 M NaOH. After establishment of a whole-cell recording, cellular capacitance was minimized by using the analog compensation available on the recording amplifier (Axopatch 200B). Series resistance was <5 MΩ and was compensated >85% in all experiments, resulting in a final series resistance no greater than 0.75 MΩ. Signals were low-pass filtered at 5–10 kHz, digitized at 20–50 kHz, and stored on a computer for later analysis. Voltage protocols were generated, and data acquisition and analysis were performed by using pCLAMP software (Version 8.1; Axon Instruments, Union City, CA). All experiments were performed at room temperature. Liquid junction potentials were <10 mV and were not corrected.

Spinal Dorsal Horn Neuronal Electrophysiology. Electrophysiological recording of spinal dorsal horn neurons was conducted as described (36). Briefly, neuropathic rats (L5–L6 spinal nerve ligation) were anesthetized with pentobarbital (50 mg/kg, i.p.), and catheters were placed in the left and right external jugular veins. A laminectomy was performed to remove vertebral segments T12-L3. The animals were then secured in a stereotaxic frame. Anesthesia was maintained for the duration of the experiment by a continuous infusion of propofol (8–12 mg/kg/hr, i.v.). Body temperature was kept at 37°C by placing the animals on a circulating water blanket. Platinum-plated stainless steel microelectrodes (Frederick Haer, Brunswick, ME) were used to record the activity of spinal wide dynamic range (WDR) neurons. Spike waveforms were monitored, digitized (32 points), and stored for offline analysis (Datawave Technologies, Longmont, CO). Baseline spontaneous activity was recorded for 5 min before stimulation. Rats were stimulated three times (5 min apart) before drug administration with a von Frey hair (10 g) applied to the neuronal receptive field for 15 s located on the ipsilateral hindpaw. The mean of three stimulations represented baseline evoked activity. A-803467 (20 mg/kg, i.v.) or vehicle was infused over a 5- to 7-min period, and the von Frey hair was reapplied 35 min after this infusion. For comparison to baseline firing levels, statistical significance was established by using Wilcoxon's matched-pairs test.

Pharmacological Selectivity Assays. The activity of A-803467 (10 μM) was evaluated in assays to assess pharmacological selectivity relative to other cell-surface receptors, ion channels, transport sites, and enzymes including the opioid receptors, and cycloxygenases 1 and 2, by use of standardized assay protocols (CEREP and in-house assays) as described (37).

Analgesia and Side-Effect Assays. A-803467 was evaluated in well characterized *in vivo* models to assess acute, inflammatory, and neuropathic pain (25, 37). The specific methodologies for these nociceptive assays, models of postoperative and visceral pain, and models of motor performance are described in the SI. Unless otherwise noted, all experimental and control groups contained at least six animals per group, and data are expressed as mean ± SEM. Data analysis was conducted by using analysis of variance and appropriate post hoc comparisons ($P < 0.05$). ED_{50} values were estimated by using least-squares linear regression.

Compound. A-803467, 5-(4-chlorophenyl)-*N*-(3,5-dimethoxyphenyl) furan-2-carboxamide (Fig. 1*A*) was synthesized at Abbott Laboratories. A-803467 was dissolved in 5% DMSO/95% polyethylene glycol (PEG 400) for i.p. administration in a 2 ml/kg injection volume. The compound was injected 30 min before behavioral testing.

We thank Mark Curran and Julie Witzel for their assistance on the molecular biology of sodium channels in the early phase of this project.

1. Waxman SG, Cummins TR, Dib-Hajj S, Fjell J, Black JA (1999) *Muscle Nerve* 22:1177–1187.
2. Goldin AL (2001) *Annu Rev Physiol* 63:871–894.
3. Yu FH, Catterall WA (2003) *Genom Biol* 4:207.
4. Lai J, Porreca F, Hunter JC, Gold MS (2004) *Annu Rev Pharmacol Toxicol* 44:371–397.
5. Renganathan M, Cummins TR, Waxman SG (2001) *J Neurophysiol* 86:629–640.
6. Coggeshall RE, Tate S, Carlton SM (2004) *Neurosci Lett* 355:45–48.
7. Tanaka M, Cummins TR, Ishikawa K, Dib-Hajj SD, Black JA, Waxman SG (1998) *NeuroReport* 9:967–972.
8. Cardenas LM, Cardenas CG, Scroggs RS (2001) *J Neurophysiol* 86:241–248.
9. England S, Bevan S, Docherty RJ (1996) *J Physiol* 495:429–440.
10. Gold MS (1999) *Proc Natl Acad Sci USA* 96:7645–7649.
11. Gold MS, Weinreich D, Kim CS, Wang R, Treanor J, Porreca F, Lai J (2003) *J Neurosci* 23:158–166.
12. Coward K, Jowett A, Plumpton C, Powell A, Birch R, Tate S, Bountra C, Anand P (2001) *NeuroReport* 12:483–488.
13. Coward K, Plumpton C, Facer P, Birch R, Carlstedt T, Tate S, Bountra C, Anand P (2000) *Pain* 85:41–50.
14. Yiangou Y, Birch R, Sangameswaran L, Eglen R, Anand P (2000) *FEBS Lett* 467:249–252.
15. Akopian AN, Souslova V, England S, Okuse K, Ogata N, Ure J, Smith A, Kerr BJ, McMahon SB, Boyce S, *et al.* (1999) *Nat Neurosci* 2:541–548.
16. Kerr BJ, Souslova V, McMahon SB, Wood JN (2001) *NeuroReport* 12:3077–3080.
17. Laird JM, Souslova V, Wood JN, Cervero F (2002) *J Neurosci* 22:8352–8356.
18. Roza C, Laird JM, Souslova V, Wood JN, Cervero F (2003) *J Physiol* 550:921–926.
19. Amir R, Argoff CE, Bennett GJ, Cummins TR, Durieux ME, Gerner P, Gold MS, Porreca F, Strichartz GR (2006) *J Pain* 7:S1–S29.
20. Nassar MA, Levato A, Stirling LC, Wood JN (2005) *Mol Pain* 1:24.
21. Khasar SG, Gold MS, Levine JD (1998) *Neurosci Lett* 256:17–20.
22. Porreca F, Lai J, Bian D, Wegert S, Ossipov MH, Eglen RM, Kassotakis L, Novakovic S, Rabert DK, Sangameswaran L, *et al.* (1999) *Proc Natl Acad Sci USA* 96:7640–7644.
23. Yoshimura N, Seki S, Novakovic SD, Tzoumaka E, Erickson VL, Erickson KA, Chancellor MB, de Groat WC (2001) *J Neurosci* 21:8690–8696.
24. Joshi SK, Mikusa JP, Hernandez G, Shieh C-C, Neelands T, Zhang X-F, Niforatos W, Kage K, Han P, Lin Z, *et al.* (2006) *Pain* 123:75–82.
25. Honore P, Jarvis MF (2006) *Comp Med Chem* 6:327–349.
26. Priestley T, Hunter JC (2006) *Drug Dev Res* 67:360–375.
27. Rush AM, Brau ME, Elliott AA, Elliott JR (1998) *J Physiol (London)* 511:771–789.
28. Cummins TR, Dib-Hajj SD, Black JA, Akopian AN, Wood JN, Waxman SG (1999) *J Neurosci* 19:RC43.
29. Zhang XF, Zhu CZ, Thimmapaya R, Choi WS, Honore P, Scott VE, Kroeger PE, Sullivan JP, Faltynek CR, Gopalakrishnan M, *et al.* (2004) *Brain Res* 1009:147–158.
30. Joshi S, Hernandez G, Mikusa J, Zhu C, Zhong C, Salyers A, Wismer C, Chandran P, Decker M, Honore P (2006) *Neuroscience* 143:587–596.
31. Ness TJ, Gebhart GF (1990) *Pain* 41:167–234.
32. Brochu RM, Dick IE, Tarpley JW, McGowan E, Gunner D, Herrington J, Shao PP, Ok D, Li C, Parsons WH, *et al.* (2006) *Mol Pharmacol* 69:823–832.
33. Stummann TC, Salvati P, Fariello RG, Faravelli L (2005) *Eur J Pharmacol* 510:197–208.
34. Gu JG, MacDermott AB (1997) *Nature* 389:749–753.
35. Amaya F, Decosterd I, Samad TA, Plumpton C, Tate S, Mannion RJ, Costigan M, Woolf CJ (2000) *Mol Cell Neurosci* 15:331–342.
36. McGaraughty S, Chu K, Faltynek CR, Jarvis MF (2006) *J Neurophysiol* 95:18–25.
37. Jarvis MF, Burgard EC, McGaraughty S, Honore P, Lynch K, Brennan TJ, Subieta A, van Biesen T, Cartmell J, Bianchi B, *et al.* (2002) *Proc Natl Acad Sci USA* 99:17179–17184.